

EXPERIMENTAL AND CALCULATED STUDY OF  
LAMINAR FLOW OF A COMPRESSIBLE GAS IN  
SHORT CHANNELS WITH COOLED WALLS

I. S. Borovkov, A. P. Byrkin,  
I. D. Vershinin, and V. M. Sankovich

UDC 532.542:532 526

The method and results are presented for an experimental determination of the pressure distribution in short cylindrical and conical channels with cooled walls during the laminar flow of a compressible gas. A calculation of this flow is made using the simplified Navier–Stokes equations and the experimental and calculated pressure distributions are compared.

It was shown in [1, 2] that the laminar flow of a compressible gas in a long channel with a smooth contour can be described by the simplified Navier–Stokes equations corresponding in form with the boundary layer equations. The laws of similarity for this flow were also established in [2]. In [3], as a result of an analysis of experimental data on the start-up of cylindrical air intakes with allowance for these laws, the hypothesis was advanced that the laminar flow in a channel of relatively short length can also be described by the simplified Navier–Stokes equations. In this report, moreover, in order to create well controlled conditions in the entrance section of the channel being studied with a Mach number less than one in this section it was proposed to place the channel in a supersonic stream and using a choke located beyond the channel to provide that mode of flow for which the shock wave is located in the entrance section of the channel. A numerical (finite-difference) method of integration of the equations mentioned above was later suggested in [4] and calculations were made of the gas flow in flat and round channels with uncooled walls.

We have attempted to study experimentally and through calculation the flow of a compressible gas in short cylindrical and conical channels with cooled walls. (The results of [3], like [4], pertain to the case of uncooled walls.)

The experiments were carried out by the method of [3] and therefore a low-density wind tunnel in the working section of which a supersonic air stream was produced was used for their performance.

The nozzle of the tunnel was conical with a diameter of 5 mm at the critical section, an aperture half-angle of  $22^\circ$ , and a diameter of 19.3 mm at the exit section.

Since in the working range of pressures  $p_0$  in the tunnel forechamber the value of  $p_0$  markedly affected the parameters of the supersonic stream beyond the nozzle cut, before conducting the main experiments the longitudinal and transverse fields of Mach numbers of this stream were determined for different values of  $p_0$ . The fields of Mach numbers were determined at the stagnation temperature  $T_0 = 576^\circ\text{K}$  since all the experiments were conducted at just this temperature.

The dependence on  $p_0$  of the distance  $[x]_{M=4.5}$  from the nozzle cut at which the same Mach number  $M = 4.5$  is attained was constructed from the longitudinal fields of Mach numbers. This was done in connection with the fact that the study of the flow in channels was designed to be conducted at a constant Mach number  $M_1$  at the entrance section of the channels. (We note that  $M_1 = 0.4236$  when  $M = 4.5$  in the case of the method used in [3].)

---

Translated from *Inzhenerno-Fizicheskii Zhurnal*, Vol. 26, No. 3, pp. 389–395, March, 1974.  
Original article submitted April 25, 1973.

© 1975 Plenum Publishing Corporation, 227 West 17th Street, New York, N.Y. 10011. No part of this publication may be reproduced, stored in a retrieval system, or transmitted, in any form or by any means, electronic, mechanical, photocopying, microfilming, recording or otherwise, without written permission of the publisher. A copy of this article is available from the publisher for \$15.00.

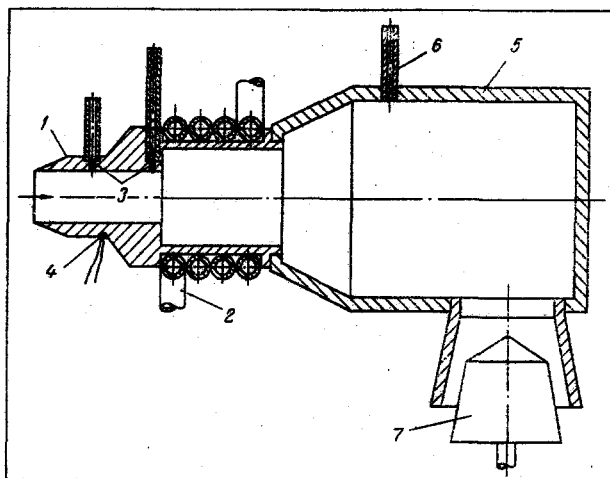


Fig. 1. Schematic diagram of model and choke chamber: 1) body of model; 2) coil; 3) drain openings; 4) thermocouple; 5) body of coke chamber; 6) tube for measurement of pressure in chamber; 7) choke.

The channels studied consisted of the inner channels of models which were placed in the supersonic stream of the tunnel in accordance with the method of [3]. The models with a choke chamber were placed on a mechanical vacuum coordinator.

A schematic diagram of the models and the choke chamber is presented in Fig. 1, where the direction of the stream impinging on the model is shown by an arrow.

Two models were used in conducting the experiments: the first with a cylindrical inner channel 6.37 mm in diameter and 20.50 mm long and the second with a conical inner channel with a diameter of 6.26 mm at the entrance section, a length of 20.55 mm, and a half-angle of taper of 0.25°.

The body 1 (Fig. 1) of each model was made of copper. The coil 2 through which water was circulated to cool the model was also made of copper and soldered to the body. Two drain openings 3, communicating with U-shaped manometers filled with silicone liquid, were made in the walls of each model. Thermocouples 4 were placed in special cavities at a distance of ~1 mm from the inner surfaces.

The drain openings served for the measurement of the static pressures  $p_{(1)}$  and  $p_{(2)}$  at the first and second measurement sections from the entrance, while the thermocouples served for the measurement of the wall temperature  $T_w$  which, like the temperature  $T_0$ , was kept constant and equal to 288°K in the experiments.

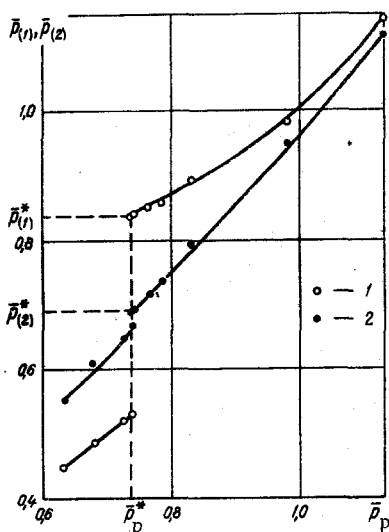


Fig. 2. Dependence of pressures in choke chamber on pressure in chamber for  $p_0 = 4.68 \cdot 10^3$  N/m<sup>2</sup>: 1)  $\bar{p}_{(1)}$ ; 2)  $\bar{p}_{(2)}$ .

The pressures  $p_{(1)}$  and  $p_{(2)}$  which are attained with different  $p_0$  when the shock wave is located in the entrance sections of the models were chosen as the experimentally determined values subject to later calculation. The method of determining these pressures, denoted below as  $p^*$ , was based on the fact [5] that the movement of the shock wave downstream from the entrance section within the model is discontinuous and is accompanied by a discontinuous decrease in  $p_{(1)}$  and  $p_{(2)}$ .

To determine  $p_{(1)}^*$  and  $p_{(2)}^*$  for some  $p_0$  this  $p_0$  and the air temperature  $T_0 = 576^\circ\text{K}$  were first set in the forechamber of the wind tunnel. Then using the coordinator the model with a closed choke chamber 5 was mounted in such a way that its entrance section was located at the distance  $[x]_{M=4.5}$ . After this the flow rate of the water cooling the model was regulated and the temperature of its walls was brought to 288°K. Then the choke 7 was gradually opened and the static pressures  $p_{(1)}$  and  $p_{(2)}$  in the first and second drain openings from the model entrance were measured, as well as the pressure  $p_p$  in the choke chamber using the tube 6. Then the

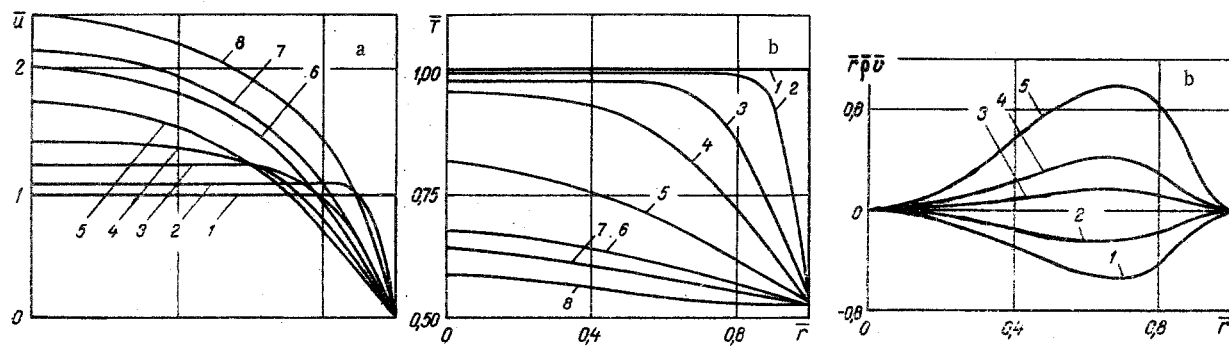


Fig. 3. Transverse profiles of  $\bar{u}$ ,  $\bar{T}$ , and  $\bar{r}\bar{\rho}\bar{v}$  for different reduced lengths  $\bar{x}$ : a and b) 1)  $\bar{x} = 0$ ; 2) 0.00146; 3) 0.01252; 4) 0.04016; 5) 0.13090; 6) 0.21930; 7) 0.23640; 8) 0.24860; c) 1)  $\bar{x} = 0.04016$ ; 2) 0.08440; 3) 0.22480; 4) 0.23650; 5) 0.24450.

dependences  $p_{(1)}(p_p)$  and  $p_{(2)}(p_p)$  were constructed which, as noted earlier, had discontinuities at the same value of  $p_p = p_p^*$  (typical dependences of  $\bar{p}_{(1)} = p_{(1)}/p_1$  and  $\bar{p}_{(2)} = p_{(2)}/p_1$  on  $\bar{p}_p = p_p/p_1$ , where  $p_1$  is the static pressure behind the direct shock wave at  $M = 4.5$ , are presented in Fig. 2). Finally, the maximum pressures  $p_{(1)}$  and  $p_{(2)}$  for  $p_p = p_p^*$ , equal to  $p_{(1)}^*$  and  $p_{(2)}^*$ , respectively, were determined.

Then a new value of  $p_0$  was set, the sequence of operations described above was repeated, new values of  $p_{(1)}^*$  and  $p_{(2)}^*$  were determined, etc.

As a result the dependences of  $p_{(1)}^*$  and  $p_{(2)}^*$  on  $p_0$  could be constructed both for models with cylindrical and with conical channels at  $M_1 = 0.424$  and  $\bar{T}_w = T_w/T_0 = 0.5$ . The Reynolds numbers  $Re_1$  corresponding to the  $p_0$ , calculated from the parameters behind the direct shock wave and the entrance section diameters of the models, varied from 56 to 124 in the case of the first model and were 65.6, 79.3, 108.9, and 138.8 in the case of the second model.†

The simplified Navier–Stokes equations mentioned above were used to calculate the flow under consideration, while the numerical method presented in [4] was used for their solution.

The system of these equations for the description of the flow of an ideal gas in an axially symmetrical channel has the following form:

$$\begin{aligned} \bar{\rho}\bar{u} \frac{\partial \bar{u}}{\partial \bar{x}} + \bar{\rho}\bar{v} \frac{\partial \bar{u}}{\partial \bar{r}} &= -\frac{d\bar{p}}{d\bar{x}} + \frac{1}{\bar{r}} \frac{\partial}{\partial \bar{r}} \left( \bar{r}\bar{\mu} \frac{\partial \bar{u}}{\partial \bar{r}} \right), \\ \frac{\partial}{\partial \bar{x}} (\bar{r}\bar{\rho}\bar{u}) + \frac{\partial}{\partial \bar{r}} (\bar{r}\bar{\rho}\bar{v}) &= 0, \\ \bar{\rho}\bar{u} \frac{\partial \bar{H}}{\partial \bar{x}} + \bar{\rho}\bar{v} \frac{\partial \bar{H}}{\partial \bar{r}} &= \frac{1}{Pr} \frac{1}{\bar{r}} \frac{\partial}{\partial \bar{r}} \left( \bar{r}\bar{\mu} \frac{\partial \bar{H}}{\partial \bar{r}} \right) \\ &- \left( \frac{1}{Pr} - 1 \right) \frac{1}{\bar{r}} \frac{\partial}{\partial \bar{r}} \left[ \bar{r}\bar{\mu} \frac{\partial (\bar{u}^2/2)}{\partial \bar{r}} \right], \\ \bar{p} &= \frac{\kappa - 1}{\kappa} \bar{\rho}\bar{h}, \quad \bar{\mu} = \bar{\mu}(\bar{h}). \end{aligned}$$

All the values in this system are dimensionless and are related to the dimensional values by the equations

$$\begin{aligned} \bar{x} &= \frac{4x}{D_1 Re_1}, \quad \bar{r} = \frac{2r}{D_1}, \quad \bar{u} = \frac{u}{u_1}, \\ \bar{v} &= \frac{v}{2u_1} Re_1, \quad \bar{p} = \frac{p}{\rho_1 u_1^2}, \quad \bar{\rho} = \frac{\rho}{\rho_1}, \quad \bar{h} = \frac{h}{u_1^2}, \quad \bar{\mu} = \frac{\mu}{\mu_1}. \end{aligned}$$

Here  $x$  is the distance along the axis of the channel from its entrance;  $r$  is the distance along the normal from the channel axis;  $u$  and  $v$  are the longitudinal and radial velocity components, respectively;  $p$  is the pressure, constant across the

†The viscosity coefficients  $\mu_1$  needed to determine the Reynolds numbers  $Re_1$  were taken from the tables of [6].

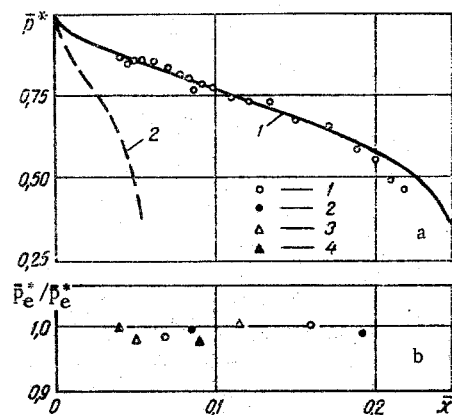


Fig. 4. Comparison of experimental and calculated values of pressures in channel. a) 1)  $\bar{T}_w = 0.5$ ; 2)  $\bar{T}_w = 1.0$ ; points: experimental values; b) 1)  $Re_1 = 65.5$ ; 2) 79.3; 3) 108.9; 4) 138.8.

channel cross section;  $\rho$  is the density;  $h$  is the enthalpy;  $H = h + u^2/2$  is the stagnation enthalpy;  $\mu$  is the viscosity coefficient;  $Pr$  is the Prandtl number;  $\kappa$  is the adiabatic index;  $D$  is the diameter of the channel section; the index 1 corresponds to the initial channel section.

The system presented was solved with the following boundary and initial conditions:

$$\begin{aligned} \frac{\partial \bar{u}}{\partial r} = \frac{\partial \bar{h}}{\partial r} = 0, \quad \bar{v} = 0 \quad \text{for} \quad \bar{r} = 0, \\ \bar{u} = \bar{v} = 0, \quad \bar{h} = \bar{h}_w = \text{const} \quad \text{for} \quad \bar{r} = \frac{2r_w}{D_1}, \\ \bar{u} = \text{const}, \quad \bar{\rho} = \text{const}, \quad \bar{h} = \text{const} \quad \text{for} \quad \bar{x} = 0. \end{aligned}$$

The initial data needed for the calculations were set in accordance with the conditions under which the experiments were conducted. For example, it was assumed that  $\kappa = 1.4$  and  $Pr = 0.71$  and an exponential dependence of the viscosity coefficient on the temperature was adopted:  $\mu \sim T^n$ ,  $n = 0.76$ . The channel walls were considered to be cooled to a constant temperature  $T_w = 0.5 T_0$ . The Mach number  $M_1$  at the channel entrance was set at 0.4236.

We note also that the dependence of  $\bar{r}_w = 2r_w/D_1$  on  $\bar{x}$  must be given when integrating the system, where  $r_w$  is the channel radius. In the present case of channels with straight generatrices this dependence has the form

$$\bar{r}_w = 1 - Re_1 \operatorname{tg} \varphi \frac{\bar{x}}{2},$$

where  $\varphi$  is the half-angle of the channel taper. From this it follows directly that in the case of a cylindrical channel ( $\varphi = 0$ ) the results of the calculations represented as a function of  $\bar{x}$  do not depend on  $Re_1$ , while conversely, in the case of a conical channel ( $\varphi \neq 0$ ) they depend on  $Re_1$ .

In connection with this, in the case of a conical channel the calculations were conducted for Reynolds numbers  $Re_1 = 65.6, 79.3, 108.9, \text{ and } 138.8$ .

In all cases the calculations were reduced practically to the critical reduced lengths  $\bar{x}$ , i.e., to the maximum channel lengths consistent with the conditions indicated above in the entrance section of the channel.

As a result of the calculations the transverse profiles  $\bar{u}(\bar{r})$ ,  $\bar{v}(\bar{r})$ , and  $T(\bar{r}) = (\bar{r})T/T_1$  at different values of  $\bar{x}$  were obtained, as well as the distributions  $\bar{p}^*(\bar{x})$  for both the cylindrical and conical channels.

The nature of the development of the transverse profiles of velocity  $\bar{u}$ , temperature  $\bar{T}$ , and the value  $\bar{\rho}\bar{v}$  in the cylindrical channel is shown in Fig. 3.

As seen from Fig. 3c, at small values of  $\bar{x}$  the transverse velocity  $\bar{v}$  is directed toward the channel axis, but as  $\bar{x}$  increases and approaches the critical value it changes sign and is directed from the channel axis toward the walls.

A comparison of the experimental and calculated distributions  $\bar{p}^*(\bar{x})$  for a cylindrical channel is presented in Fig. 4a, while the experimental and calculated values of  $\bar{p}^*$  for a conical channel are presented in Fig. 4b.†

It can be concluded from this comparison that the simplified Navier–Stokes equations used, which coincide in form with boundary layer equations, are also feasible for the description of flow in short channels with cooled walls.

In conclusion it should be mentioned that it is seen from Fig. 4a, where in addition to the distribution  $\bar{p}^*(\bar{x})$  for  $\bar{T}_w = 0.5$  the corresponding distribution is presented for  $\bar{T}_w = 1.0$  (dashed curve), that the cooling of the channel walls has a very marked effect on the flow within the channel. In particular, at  $\bar{x} = 0.04$  the relative pressure  $\bar{p}^*$  is almost 1.4 times greater for  $\bar{T}_w = 0.5$  than for  $\bar{T}_w = 1.0$ , while the critical reduced length  $\bar{x}$  of the channel for  $\bar{T}_w = 0.5$  is almost four times greater than this length for  $\bar{T}_w = 1.0$ .

†All the values of  $\bar{p}^*$  obtained were used to construct the experimental distribution  $\bar{p}^*(\bar{x})$  for the cylindrical channel since the corresponding calculated distribution does not depend on the Reynolds number  $Re_1$ .

## NOTATION

M	is the Mach number;
Re	is the Reynolds number;
$\mu$	is the viscosity coefficient;
$\kappa$	is the ratio of specific heat capacities;
D	is the diameter of channel cross section;
x	is the distance from entrance section of channel;
r	is the distance from channel axis;
p	is the pressure;
T	is the temperature;
$\rho$	is the density;
u, v	are the velocity components;
h	is the enthalpy.

### Subscripts

0	denotes the forechamber;
1	denotes the entrance section of channel;
(1), (2)	denote the first and second measurement sections from entrance.

### LITERATURE CITED

1. J. C. Williams, AIAA J., 1, 186 (1963).
2. A. P. Byrkin and I. I. Mezhirova, Izv. Akad. Nauk SSSR, Mekhan. Zhidk. i Gaza, No. 6, 156 (1967).
3. I. S. Borovkov, I. D. Vershinin, and Yu. G. Rakogon, Uch. Zap. Tsentr. Aero-Gidrodin. Inst., 4, No. 1, 97 (1973).
4. A. P. Byrkin, *ibid.*, 4, No. 5, 62 (1973).
5. I. S. Borovkov, I. D. Vershinin, and Yu. G. Rakogon, Proceedings of First Lectures Devoted to the Exploitation of the Scientific Heritage and Development of the Ideas of F. A. Tsander. II. Theory and Construction of Engines [in Russian], Znanie, Moscow (1972), p. 93.
6. N. B. Vargaftik, Handbook on Thermophysical Properties of Gases and Liquids [in Russian], GIFML, Moscow (1963).